

Article

Experimental Study on Flexural Behavior of RC–UHPC Slabs with EPS Lightweight Concrete Core

Tuan-Anh Cao, Manh-Tuan Nguyen, Thai-Hoan Pham and Dang-Nguyen Nguyen * 

Faculty of Building and Industrial Construction, Hanoi University of Civil Engineering, 55 Giai Phong, Hai Ba Trung, Hanoi 100000, Vietnam; anhct@huce.edu.vn (T.-A.C.); tuannm1@huce.edu.vn (M.-T.N.); hoanpt@huce.edu.vn (T.-H.P.)

* Correspondence: nguyennnd@huce.edu.vn; Tel.: +84-(91)-2031288

Abstract: This paper presents an experimental investigation that focuses on the flexural behavior of an innovative reinforced concrete–ultra-high performance concrete slab with an expanded polystyrene lightweight concrete core. This type of slab is proposed to serve the semi-precast solution, in which the bottom layer is ultra-high performance concrete working as a formwork during the construction of semi-precast slab, the expanded polystyrene lightweight concrete layer is used for the reduction of structure self-weight, and the top layer is normal concrete designed to withstand compressive stress when the slab is loaded. Two similar large-scale specimens with dimensions of 6200 mm × 1000 mm × 210 mm were fabricated and tested under four-point bending conditions to investigate the flexural behavior of composite slab. Test results indicated that three different layers of materials can work effectively together without separation. The bottom ultra-high performance concrete layer leads to the high ductility of the slab and has a good effect in limiting the widening of the crack width by forming other cracks. According to design code ACI 544.4R, a modified distribution stress diagram on the composite section was proposed and proven to be suitable for the prediction of flexural strength of the composite section with an error of 3.4% compared to the experimental result. The effect of the ultra-high performance concrete layer on the flexural strength of the composite slab was clearly demonstrated, and for the case in this study, the ultra-high performance concrete layer improves the flexural strength of the slab by about 11.5%.

Keywords: flexural behavior; reinforced concrete–ultra-high performance concrete slab; expanded polystyrene lightweight concrete; four-point bending test



Citation: Cao, T.-A.; Nguyen, M.-T.; Pham, T.-H.; Nguyen, D.-N.

Experimental Study on Flexural Behavior of RC–UHPC Slabs with EPS Lightweight Concrete Core.

Buildings **2023**, *13*, 1372. <https://doi.org/10.3390/buildings13061372>

Academic Editors: Quang-Viet Vu, Viet-Hung Truong and George Papazafeiropoulos

Received: 13 April 2023

Revised: 16 May 2023

Accepted: 22 May 2023

Published: 24 May 2023



Copyright: © 2023 by the authors. Licensee MDPI, Basel, Switzerland. This article is an open access article distributed under the terms and conditions of the Creative Commons Attribution (CC BY) license (<https://creativecommons.org/licenses/by/4.0/>).

1. Introduction

Reinforced concrete (RC) is the most commonly used material for construction worldwide. Formwork made from wood or steel has the temporary function of shaping and fixing fresh concrete to fabricate RC members and structures, which is removed when concrete hardens. The processes of installing and removing the temporary formwork create a considerable amount of solid waste at the construction site and spend significant resources in terms of construction cost and time. Therefore, precast RC has attracted much attention from researchers investigating and developing methods of reducing construction waste, shortening construction time, and decreasing construction cost effectively, with the aim of sustainable construction [1]. Many studies have analyzed the cost and time advantages of precast concrete construction systems compared to conventional construction and reported that up to 40% of cost and time can be saved by appropriate planning and implementation in precast constructions [2,3]. As an inevitable consequence, the research and development of precast concrete structures has increased rapidly in the past few decades [1,4–6]. A semi-precast reinforced concrete slab, as an innovative precast concrete member, comprises a bottom precast RC layer (precast plank) and a cast in situ concrete topping. Problems with concrete topping and continuous reinforcement between

the slab unit and the supporting component have been well described and considered through numerical and experimental modeling in a recent study [7]. The contact surface between the layers is usually roughened to enhance the bonding between different material layers. In addition, in some cases, inclined steel truss bars have penetrated the interface to stiffen the precast plank as well as improve the composite action of the entire slab [8]. With this type of slab structure, the bottom precast plank is used as the formwork during the fabrication of such semi-precast structures. Therefore, the cost of formwork can be minimized. Deng et al. [9] synthesized other investigations [8,10–13] and showed that the precast RC composite slab with inclined steel truss bars acquires beneficial features of both precast and RC slabs cast in situ, containing high construction efficiency and cost savings, high integrity, high reliability, and comparable mechanical behavior to that of popular slabs cast in situ. These studies also pointed out that the inclined steel truss bars have an insignificant impact on the load-carrying capacity but can greatly improve the ductility of the RC composite slab. The influences of different steel truss bars and innovative joint configurations on the flexural bending tests of composite slabs have been examined [11,13].

The self-weight of the structural floor system accounts for a large proportion of the total dead load in reinforced concrete buildings [14]. The self-weight of floor structural slabs typically possesses approximately 40–60% of the entire structure mass, according to a simple calculation for loads of a residential high-rise building, and a 10% reduction in slab self-weight can lead to a 5% reduction in total building self-weight [15]. The lighter self-weight of the structural slab reduces seismic response, resulting in lower bearing capacity demands for main structural components such as shear walls, columns, and beams [16]. The lightweight slab could make lifting and installation easier during precast concrete slab construction, resulting in significant cost savings and accident reduction [17–19]. Moreover, the semi-precast concrete slab is prone to cracking during the lifting and installation process because of the low tensile strength of normal concrete, leading to the low durability concern of the structure during service. Thus, a solution for a lightweight semi-precast composite slab with high cracking resistance and tensile bearing capacity is necessary.

Concerning the idea of combining lightweightness and high tensile performance of precast plank, an innovative reinforced concrete-ultra high-performance concrete (RC-UHPC) slab with expanded polystyrene (EPS) lightweight concrete core (so-called RC-UHPC composite slab) is proposed to serve the semi-precast solution. For this type of composite slab, the bottom layer of ultra-high-performance concrete (UHPC) with an inclined steel truss bars system works as a formwork during the construction of a semi-precast slab, the EPS lightweight concrete layer is used for the reduction of structure self-weight, and the top layer is normal concrete designed to withstand compressive stress when the slab is loaded. UHPC has high compressive (up to 150 MPa) and especially tensile strengths (up to 15 MPa), which are much higher than normal concrete. The high density and compactness of the UHPC matrix lead to great physical performance as low permeability can restrain the access of negative substances, leading to enhanced durability [20,21]. UHPC also exhibits other outstanding characteristics including high energy dissipation, fracture energy (up to 40 kJ/m²), and ductility [22]. An additional interesting characteristic is the strain-hardening performance of UHPC in tension owing to the presence of steel fibers [23]. Considering the excellent physical and mechanical performance of UHPC, this material is used for the proposed RC-UHPC composite slab, as several previous studies have successfully implemented [24,25]. For the lightweight infill material of the slab, expanded polystyrene (EPS) lightweight concrete that has been utilized for several decades to reduce the structural weight is adopted. Besides reducing the structure's self-weight, EPS concrete also revealed good functional uses such as sound and thermal insulation [26].

For the application of the proposed RC-UHPC composite slab in practice, several related issues need to be investigated, in which two important issues are as follows: (i) the ability to work effectively together as a composite slab (composite action) considering the different fabrication time of different material layers; and (ii) the load carrying capacity

of the entire composite slab and how to design this type of slab. The former will be solved by the design of inclined truss bars in a future work, while the latter is investigated in this study. For this purpose, two large-scale specimens with the same dimensions of $6200 \times 1000 \times 210$ mm were fabricated and tested according to a four-point bending scheme to investigate the flexural behavior of the proposed RC–UHPC composite slab. According to design code ACI 544.4R, a modified distribution stress diagram on RC–UHPC composite section was also proposed and proven to be suitable for the prediction of the flexural strength of the RC–UHPC composite section.

2. Experimental Program

2.1. Specimen Dimensions

Two specimens—namely, M1 and M2—were designed to investigate the flexural behavior of the proposed RC–UHPC composite slabs with EPS lightweight concrete cores (so-called RC–UHPC composite slabs). The specimens have the same rectangular cross-section with the dimension of $6200 \times 1000 \times 210$ mm. This is the actual size of the slab plate that will be used in the semi-precast slab structure. The cross-sectional thickness of RC–UHPC slabs consist of 3 different layers of materials. The bottom layer is UHPC with a thickness of 30 mm, the middle layer is expanded polystyrene (EPS) lightweight concrete with a thickness of 120 mm, and the top layer is normal concrete (NC) with a thickness of 60 mm. These thicknesses of material layers were designed with minimum UHPC layer thickness and maximum EPS lightweight concrete layer thickness to minimize the cost and self-weight of the slab structure.

For the purposes of using the bottom layer of UHPC as formwork during the construction of the semi-precast slab, the lightweight concrete layer for the reduction of structure self-weight, and the top layer of normal concrete for the subjection of compressive stress when the slabs are bearing, the reinforcement of RC–UHPC composite slab includes three main components: the bottom mesh, the inclined transverse reinforcements, and the top mesh. The bottom mesh consists of the main longitudinal rebars of 10 mm diameter, with a spacing of 180 mm and distribution rebars of 6 mm diameter. This mesh is embedded in the UHPC layer with a cover layer of 10 mm. The inclined transverse reinforcements with a diameter of 6 mm are used not only to connect the UHPC and NC layers but also to serve the lifting process of the UHPC bottom plate during the construction of the semi-precast slab. The top mesh consists of three main longitudinal rebars with a diameter of 10 mm, which directly connect to the inclined reinforcements and the additional distribution rebars of 6 mm diameter in both directions to form a reinforcing mesh that meets constructive requirements. This mesh is embedded in the NC layer with a cover layer of 20 mm. The dimensions and reinforcement details of the test specimens are illustrated in Figure 1.

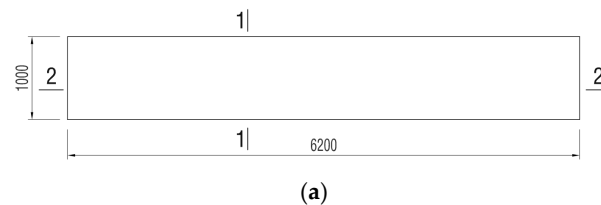
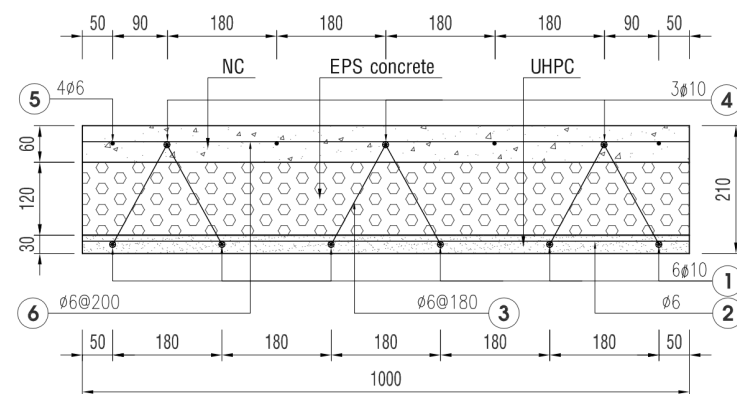
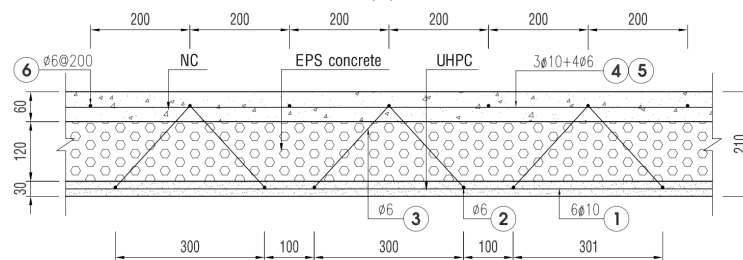


Figure 1. Cont.



Section 1-1

(b)



Section 2-2

(c)



(d)

Figure 1. Dimensions (in mm) and reinforcement details of the test specimens: (a) dimensions of the test specimens; (b) cross section of specimens and reinforcement details; (c) longitudinal section of specimens and reinforcement details; (d) installation of reinforcements.

2.2. Materials

The raw materials of UHPC consist of quartz sand with an average diameter of 300 μm , cement Type I, silica fume (SF) with an average diameter of 0.15 μm , steel fiber with a volume fraction of 1%, and polycarboxylate-based superplasticizer (SP) additive. The

composition of raw materials for 1 m³ of UHPC mixture is listed in Table 1, and the physical and mechanical properties of steel fiber are shown in Table 2.

Table 1. Mix proportion of UHPC.

| Amount of Raw Materials for 1 m ³ of UHPC | | | | | |
|--|------------|-------------|------------------|------------------|----------------------|
| Fiber (kg) | Water (kg) | Cement (kg) | Silica Fume (kg) | Quartz Sand (kg) | Superplasticizer (%) |
| 79 | 163 | 895 | 224 | 1120 | 39.8 |

Table 2. Properties of steel fiber.

| d_f (mm) | L_f (mm) | ρ (g/cm ³) | f_t (MPa) | E_f (GPa) |
|------------|------------|-----------------------------|-------------|-------------|
| 0.15 | 15 | 7.9 | 2500 | 200 |

Notes: d_f ; L_f ; ρ ; f_t ; E_f are the diameter, length, density, tensile strength, and elastic modulus of the steel fiber, respectively.

The mix proportion of normal concrete was designed to obtain concrete with a compressive strength of around 35 MPa, as shown in Table 3.

Table 3. Mix proportion of normal concrete (1 m³).

| Cement (kg) (m ³) | Stone (kg) (m ³) | River Sand (kg) (m ³) | Water (kg) (m ³) |
|----------------------------------|---------------------------------|--------------------------------------|---------------------------------|
| 455 | 1197 | 575 | 200 |
| −0.406 | −0.818 | −0.392 | −0.2 |

The EPS concrete used expanded polystyrene beads with the size of 3–4 mm and Sikament R4 plasticizer as an additive. The mix proportion of EPS concrete was designed to obtain concrete with a density of about 1200 kg/m³, as shown in Table 4.

Table 4. Mix proportion of EPS concrete (1 m³).

| Cement (kg) | Sand (kg) | Additive (kg) | Water (kg) | EPS Beads (kg) |
|-------------|-----------|---------------|------------|----------------|
| 350 | 245 | 4.4 | 120 | 4 |

The mechanical properties of concrete materials were determined from the test results of specimens according to ASTM standards after 28-day curing age. For compressive strength of each concrete type, three cylindrical specimens with the size of 100 mm × 200 mm were prepared and tested according to ASTM C39M [27], while three cylindrical specimens with the same size were prepared and tested according to ASTM C469M [28] for the elastic modulus. The compressive strength and elastic modulus of each concrete type were taken as the average value of three values from the corresponding tests. As a result, the UHPC has a compressive strength of $f_{ck,UHPC} = 123.7$ MPa and an elastic modulus of $E_{UHPC} = 42.5$ GPa; the NC has a compressive strength of $f_{ck} = 34.66$ MPa and an elastic modulus of $E_{NC} = 33.20$ GPa; and the EPS concrete has a compressive strength of $f_{ck,EPS} = 3.68$ MPa and an elastic modulus of $E_{EPS} = 3.35$ GPa. The density of UHPC, normal concrete, and EPS concrete were also measured to be 2645 kg/m³, 2340 kg/m³, and 1180 kg/m³, respectively. Longitudinal, inclined, and transverse reinforcements of the PC-UHPC slab specimens consist of two types of rebars with diameters of 10 mm and 6 mm that have yielding strengths of 420.7 MPa and 315.5 MPa. The UHPC tensile strength test was not conducted for the batch that was used to fabricate the RC-UHPC specimen due to the limited testing conditions at that time. However, the tensile strength test of the same UHPC mix proportion with another batch had been conducted before. Figure 2 shows the stress–strain curves obtained from the axial tensile test of 3 dog bone-shaped UHPC

specimens with the same cross-section of 25×50 mm and a gauge length of 175 mm. The average tensile strength of the UHPC from the three tests is 8.37 MPa.

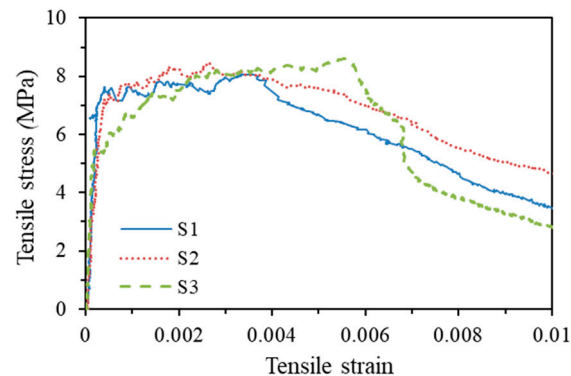


Figure 2. Stress–strain behavior of UHPC.

2.3. RC–UHPC Specimen Preparation and Test Setup

All materials were prepared and the RC–UHPC specimens were fabricated in the laboratory. High-quality wood formworks were utilized and the reinforcement diagram, which was separately tied, was installed into the formworks first. Each concrete type was thoroughly mixed in compliance with specifications and then poured into the formwork with design thicknesses in the order of UHPC, EPS, and normal concrete from the bottom up. After fabrication, two specimens were cured at room temperature and humidity for 28 days until testing. The processes for the fabrication of RC–UHPC composite specimens are shown in Figure 3.

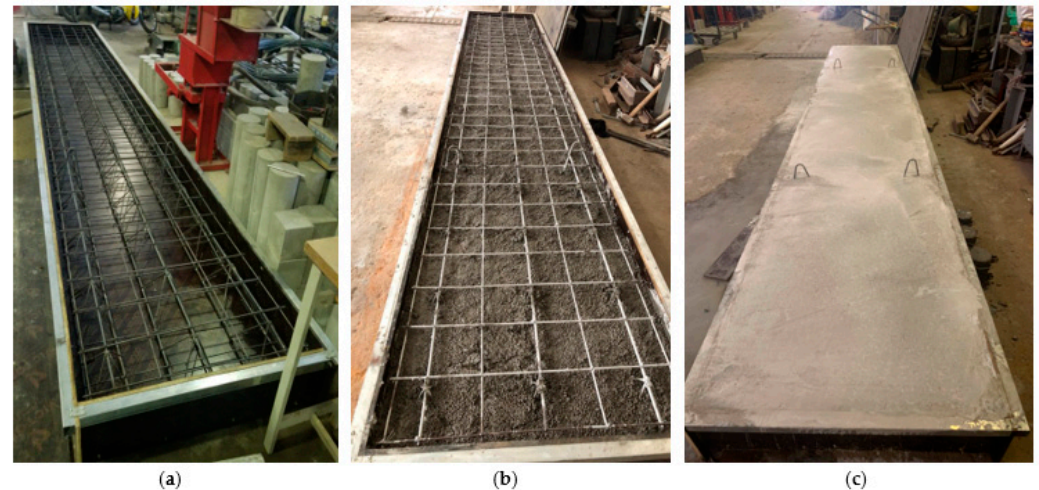


Figure 3. Fabrication of RC–UHPC composite specimen: (a) installation of reinforcement diaphragm into formworks; (b) after pouring EPS concrete layer; (c) after pouring NC layer.

The bending behavior of the specimens was investigated by a four-point bending test under monotonic loading. The 6200 mm length specimen was placed on two simple supports with a clear span of 6000 mm; one end is hinged support and the other end is roller support with a distance of 100 mm from the edges of the test specimen. Two symmetrical concentrated loads at a distance of 2250 mm from the nearest support were applied to the test specimens through two steel spreader beams placed above to distribute the load to the test specimens, leading to the length of a maximum bending moment of 1500 mm. The loads were generated by a servo-hydraulic actuator with the maximal measuring range of 1000 kN. During the experiment, the applied load was measured by a load cell. The mid-span vertical displacement at each applied load level was measured by installing three linear variable displacement transducers (LVDTs). Two displacement

and some of the largest cracks had grown into the normal concrete layer. No separation of different concrete layers was observed during the test. These results indicate that the UHPC layer has a good effect in limiting the widening of the crack width by forming other cracks, unlike normal concrete, as shown in the literature [1,29]. In addition, the bonding between the concrete layers is very good, allowing different layers of materials to work simultaneously. However, this issue needs to be further studied when the layers of material are poured at different times. In summary, ductile flexural failure occurred in both specimens without concrete crushing in the compression zone. The typical failure mode and crack distribution of the RC–UHPC composite slab specimen are shown in Figure 5.



Figure 5. (a) Failure mode and (b) crack distribution of specimen M1.

Figure 6 shows the applied load versus mid-span deflection relationships for both specimens, M1 and M2. In this figure, the flexural cracking, yielding, and ultimate points are also plotted, while the corresponding load values at these stages are listed in Table 5. As can be seen in Figure 6, the load–deflection curves of the two specimens display the same pattern. A linear relationship is observed before the crack occurs and the curves almost keep linear after that, with only a slight decrease in stiffness. When the longitudinal reinforcement yields, the stiffness of both specimens drops with a long ductile plateau stage before failure. The high ductility of specimens exhibited over the long ductile plateau stage in the case of a rather low longitudinal reinforcement ratio of 0.24% is attributed to the UHPC layer as indicated in literature [30].

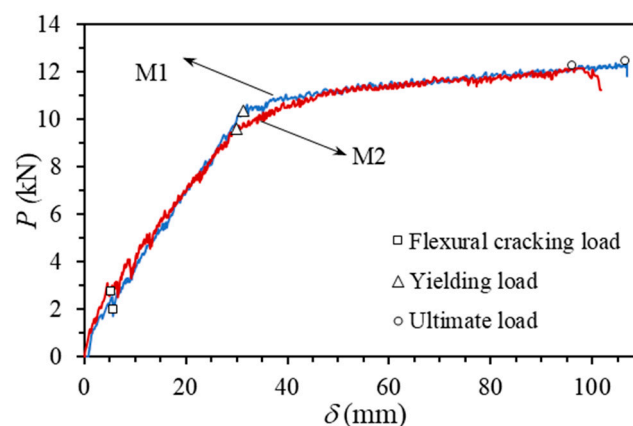


Figure 6. Load–deflection curves of RC–UHPC composite slab specimens.

Table 5. Applied load P at different stages.

| Specimen | Cracking Load (kN) | Yielding Load (kN) | Ultimate Load (kN) |
|----------|--------------------|--------------------|--------------------|
| M1 | 1.98 | 10.33 | 12.43 |
| M2 | 2.75 | 9.60 | 12.25 |

The relationships between the applied load and strain at the middle of each concrete layer at the mid-span section of specimens M1 and M2 are shown in Figure 7, in which the positive value denotes the tensile strain, while the negative value characterizes the compressive strain. As seen in this figure, the measured results have some abnormality; it is possible that the strain gauges are only installed on one side of the test specimens, resulting in uncertain measurement results. However, the similar results of the tensile strain at the middle of the UHPC layer from two specimens indicate that the measured strain from ST-3 may be reliable. Based on these measured results, the large tensile strain in the middle of the UHPC layer of about $4000 \mu\epsilon$ demonstrates, once again, the effect of this layer on the ductility of the RC–UHPC composite slabs.

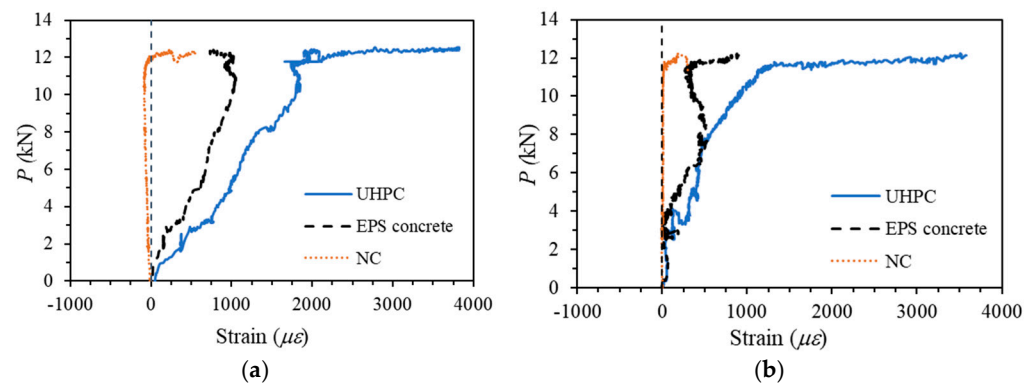


Figure 7. Load–strain relationship of concrete layers at the mid–span section. (a) Specimen M1; (b) Specimen M2.

4. Flexural Strength of RC–UHPC Composite Section

According to the test results, the flexural strength of the RC–UHPC composite section can be determined using the following equation:

$$M = Pl_1 + \frac{sw}{8}L^2 \quad (1)$$

where l_1 is the distance from the load position P to the nearest support in Figure 4 ($l_1 = 2.25$ m); L is the span of the test specimen ($L = 6.0$ m); and sw is the self-weight uniformly distributed over the length of the specimen. From the measured density of each material layer in the RC–UHPC composite slab and the obtained ultimate load, the flexural strength of the RC–UHPC composite section was calculated to be 44.01 kN·m and 43.66 kN·m for M1 and M2 specimens, respectively.

The current design codes do not mention the bearing capacity of flexural members with the composite cross-section as in this study; they only refer to the calculation of the reinforced concrete or reinforced UHPC cross-section; for example, the ACI codes system. In this study, the ACI codes are used to predict the flexural strength of the RC–UHPC composite section to check whether these standards are suitable for determining the flexural capacity of composite cross-sections. Current design code ACI 318 [31] uses the strain diagram and simplified stress distribution as presented in Figure 8a and implies that the flexural strength of reinforced concrete section can be computed by the following:

$$M_n = A_s f_y \left(d - \frac{a}{2} \right) \quad (2)$$

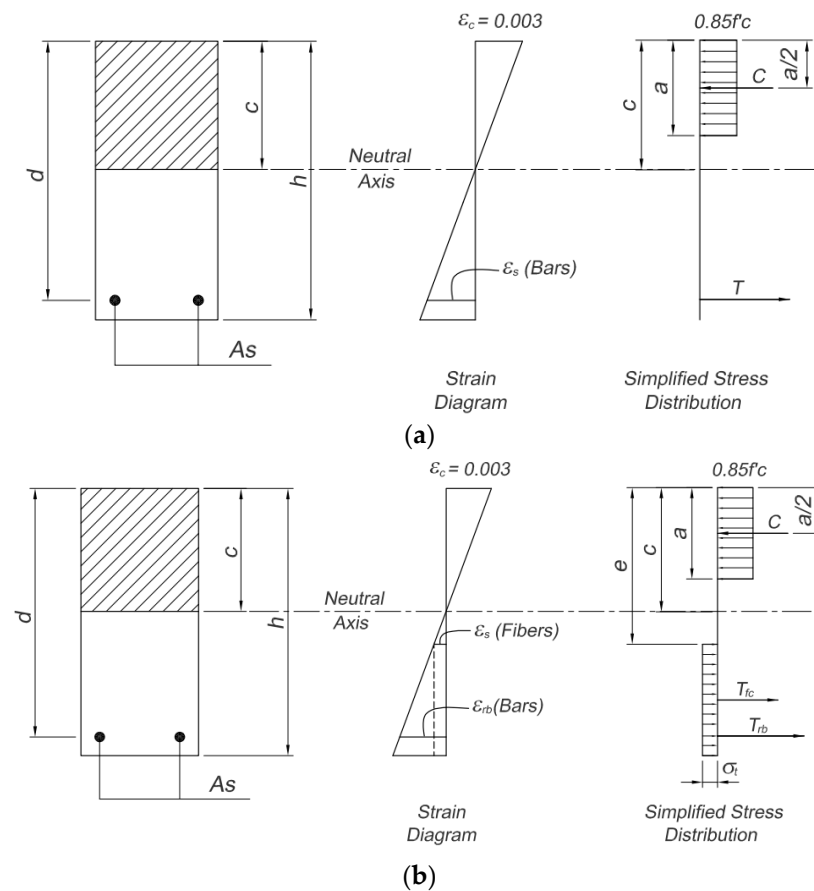


Figure 8. Stress–strain distribution of bending section in ACI codes. (a) ACI 318 for reinforced concrete [31]; (b) ACI 544.4R for steel fiber-reinforced concrete [32].

In Equation (2), a is the depth of the rectangular stress block that can be determined as $a = \beta_1 c$, where β_1 is the stress block parameter and c is the neutral axis depth. For compressive strength of concrete between 17 and 28 MPa, $\beta_1 = 0.85$, β_1 shall be reduced linearly with a rate of 0.05 for every 7 MPa of compressive strength of concrete above 28 MPa, and the smallest value of β_1 is 0.65. As can be seen in this equation and Figure 8, the ACI 318 design code [31] neglects the capacity of concrete in the tensile zone. However, for a steel fiber reinforced concrete section or composite section with a layer of steel fiber concrete in the tensile zone, the effect of steel fiber should be considered. For flexural strength of the steel fiber-reinforced concrete section, the ACI 544.4R code [32] adopts the strain diagram and simplified stress distribution as presented in Figure 8b and provides the flexural strength equations as follows:

$$M_n = A_s f_y \left(d - \frac{a}{2} \right) + \sigma_t b (h - e) \left(\frac{h}{2} + \frac{e}{2} - \frac{a}{2} \right) \quad (3)$$

where,

M_n is the nominal flexural strength of the section;

f_y is the yield strength of steel rebar;

d is the effective depth of the section;

a is the depth of stress block;

b is the width of the section;

h is the height of the section;

$e = [\epsilon_s(\text{fibers}) + 0.003] c / 0.003$ where $\epsilon_s(\text{fiber}) = \sigma_f / E_s$;

c is the neutral axis depth;

and σ_t is the tensile stress in fibrous concrete, which can be calculated as follows:

$$\sigma_t = 0.00772 \frac{l_f}{d_f} \rho_f F_{be} \quad (4)$$

where l_f is the length of steel fiber; d_f is the diameter of steel fiber; ρ_f is the percent by volume of steel fiber; and F_{be} is the bond efficiency factor which varies from 1.0 to 1.2 depending upon fiber characteristics. Thus, the effect of steel fiber in the tensile zone is considered through the tensile force of fibrous concrete, which is as follows:

$$T_{fc} = \sigma_t b (h - e) \quad (5)$$

With the RC–UHPC composite slab proposed in this study, the thickness of normal concrete is always designed to adequately carry the compressive force when the cross-section is in the limit state. The effect of EPS concrete on the flexural strength of the section can be neglected due to its very low strength in both compression and tension. Therefore, if the tensile strength of the UHPC layer is not taken into account, the flexural strength of the composite section can be calculated as the normal reinforced concrete section according to ACI 318 [31] by using Equation (2). In case the effect of steel fiber in the tensile zone is considered, meaning that the tensile strength of the UHPC layer is taken into account, the stress distribution on the RC–UHPC composite section can be simplified as shown in Figure 9. In this model, the tensile stress is uniformly distributed in the whole thickness of the UHPC layer (t_{UHPC}) with the value of σ_t as in Equation (4) if $t_{UHPC} \leq e$, where e is determined according to ACI 544.4R [32], considering the entire tension zone of the section as UHPC. In the opposite case, $t_{UHPC} > e$, the stress distribution in Figure 8b is adopted.

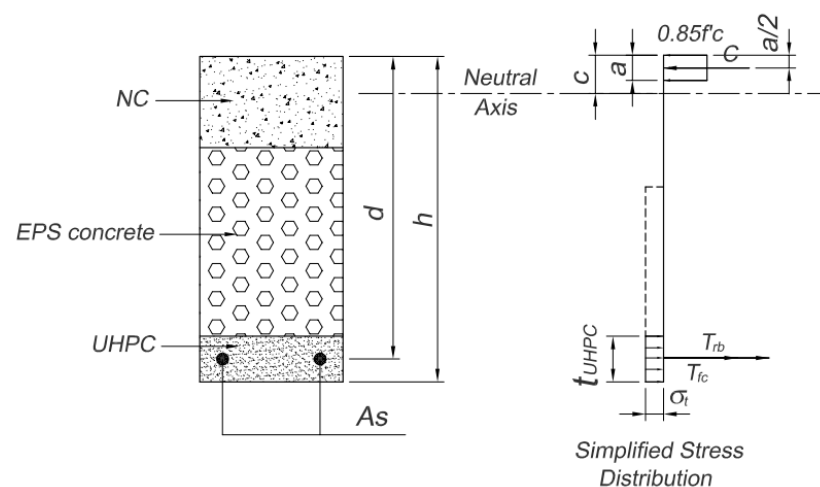


Figure 9. Stress distribution of RC–UHPC bending section.

The flexural strengths of the RC–UHPC composite section according to the aforementioned cases were calculated and are presented in Table 6, together with their relative error from the experimental results where the experimental value is the mean of the two specimens. The used material parameters for calculation are $f'_c = 34.66$ MPa, $A_s = 471.2$ mm² ($6\phi 10$), $f_y = 420.7$ MPa, $d_f = 0.15$ mm, $l_f = 15$ MPa, $\rho_f = 1\%$, $F_{be} = 1.0$, and $\beta_1 = 0.803$, while the section parameters are $b = 1000$ mm, $h = 210$ mm, $d = 195$ mm, and $t_{UHPC} = 30$ mm. The depth of the stress block was calculated to be 6.73 mm when the tensile strength of the UHPC layer is not taken into account (ACI 318 [31]), and to be 7.52 mm when the tensile strength of the UHPC layer is considered (ACI 544.4R [32]).

Table 6. Flexural strength of RC–UHPC composite according to experiment and ACI design codes.

| Experiment M (kN·m) | ACI 318 [31] | | ACI 544.4R [32] | |
|--------------------------|--------------|-----------|-----------------|-----------|
| | M_n (kN·m) | Error (%) | M_n (kN·m) | Error (%) |
| 43.83 | 37.99 | 13.3 | 42.34 | 3.4 |

As can be seen in Table 6, the flexural strength of the RC–UHPC composite section predicted using ACI 318 [31] is somewhat lower than the experimental result with a relative error of 13.3%, while ACI 544.4R using the proposed distribution stress diagram shows much better-predicted strength, with a small relative error of 3.4%. Thus, the effect of the UHPC layer on the flexural strength of the RC–UHPC composite slab is clearly demonstrated; for the case of the designed composite section in this study, the UHPC layer improves the flexural strength of the slab by about 11.5%. The obtained result also indicates that ACI 544.4R [32], with the modified distribution stress diagram as presented in Figure 8, is suitable for the prediction of flexural strength of the RC–UHPC composite section.

5. Conclusions

In this study, the flexural behavior of innovative RC–UHPC composite slabs under a four-point bending scheme was studied. The effects of the bottom UHPC layer of the composite section were investigated. The test results support the following conclusions:

1. Three different layers of materials can work effectively together without separation when the inclined transverse steel reinforcement is introduced and the layers of material are poured continuously. This issue needs to be further studied when the layers of material are poured at different times;
2. The bottom UHPC layer can lead to the high ductility of the slab and has a good effect in limiting the widening of the crack width by forming other cracks;
3. According to design code ACI 544.4R, a modified distribution stress diagram on the RC–UHPC composite section was proposed and has been proven to be suitable for the prediction of flexural strength of the RC–UHPC composite section, with an error of 3.4% compared to the experimental result;
4. The effect of the UHPC layer on the flexural strength of the composite slab was clearly demonstrated, and for the case in this study, the UHPC layer improves the flexural strength of the slab by about 11.5%.

It is noted that the aforementioned conclusions are based on a very limited number of experiments and are indicative.

For the application of the proposed RC–UHPC composite slab in practice, a very important issue, which is the ability to work effectively together as a composite slab (composite action), considering the different fabrication time of different material layers, needs to be comprehensively investigated. This issue will be dealt with in future work.

Author Contributions: Conceptualization, T.-A.C. and M.-T.N.; methodology, T.-A.C. and T.-H.P.; software, T.-H.P.; validation, T.-A.C., M.-T.N., T.-H.P. and D.-N.N.; formal analysis, T.-A.C. and T.-H.P.; investigation, T.-H.P.; resources, M.-T.N. and T.-H.P.; data curation, T.-H.P. and D.-N.N.; writing—original draft preparation, D.-N.N.; writing—review and editing, T.-H.P.; visualization, D.-N.N.; supervision, M.-T.N.; project administration, T.-A.C.; funding acquisition, T.-A.C. All authors have read and agreed to the published version of the manuscript.

Funding: This research was funded by the Ministry of Education and Training of Vietnam, grant number B2020-XDA-06.

Data Availability Statement: The data presented in this study are available on request from the corresponding author.

Conflicts of Interest: The authors declare no conflict of interest.

References

1. Mohamed, M.I.S.; Thamboo, J.A.; Jeyakaran, T. Experimental and Numerical Assessment of the Flexural Behaviour of Semi-Precast-Reinforced Concrete Slabs. *Adv. Struct. Eng.* **2020**, *23*, 1865–1879. [\[CrossRef\]](#)
2. Shen, L.; Tam, V.W.; Li, C. Benefit Analysis on Replacing in Situ Concreting with Precast Slabs for Temporary Construction Works in Pursuing Sustainable Construction Practice. *Resour. Conserv. Recycl.* **2009**, *53*, 145–148. [\[CrossRef\]](#)
3. Akmam Syed Zakaria, S.; Gajendran, T.; Rose, T.; Brewer, G. Contextual, Structural and Behavioural Factors Influencing the Adoption of Industrialised Building Systems: A Review. *Archit. Eng. Des. Manag.* **2018**, *14*, 3–26. [\[CrossRef\]](#)
4. Xu, Q.; Chen, L.; Li, X.; Han, C.; Wang, Y.C.; Zhang, Y. Comparative Experimental Study of Fire Resistance of Two-Way Restrained and Unrestrained Precast Concrete Composite Slabs. *Fire Saf. J.* **2020**, *118*, 103225. [\[CrossRef\]](#)
5. Lam, S.S.E.; Wong, V.; Lee, R.S.M. Bonding Assessment of Semi-Precast Slabs Subjected to Flexural Load and Differential Shrinkage. *Eng. Struct.* **2019**, *187*, 25–33. [\[CrossRef\]](#)
6. Adawi, A.; Youssef, M.A.; Meshaly, M.E. Experimental Investigation of the Composite Action between Hollowcore Slabs with Machine-Cast Finish and Concrete Topping. *Eng. Struct.* **2015**, *91*, 1–15. [\[CrossRef\]](#)
7. Sarkis, A.I.; Sullivan, T.J.; Brunesi, E.; Nascimbene, R. Investigating the Effect of Bending on the Seismic Performance of Hollow-Core Flooring. *Int. J. Concr. Struct. Mater.* **2023**, *17*, 18. [\[CrossRef\]](#)
8. Liu, Y.L.; Huang, J.Q.; Chong, X.; Ye, X.G. Experimental Investigation on Flexural Performance of Semi-Precast Reinforced Concrete One-Way Slab with Joint. *Struct. Concr.* **2021**, *22*, 2243–2257. [\[CrossRef\]](#)
9. Deng, B.-Y.; Tan, D.; Li, L.-Z.; Zhang, Z.; Cai, Z.-W.; Yu, K.-Q. Flexural Behavior of Precast Ultra-Lightweight ECC-Concrete Composite Slab with Lattice Girders. *Eng. Struct.* **2023**, *279*, 115553. [\[CrossRef\]](#)
10. Du, H.; Hu, X.; Meng, Y.; Han, G.; Guo, K. Study on Composite Beams with Prefabricated Steel Bar Truss Concrete Slabs and Demountable Shear Connectors. *Eng. Struct.* **2020**, *210*, 110419. [\[CrossRef\]](#)
11. Kanchanadevi, A.K.; Ramanjaneyulu, K.; Srinivas, V. Behaviour of Concrete Composite Slabs with Truss Type Shear Connectors of Different Orientation Angle. *Adv. Struct. Eng.* **2021**, *24*, 3070–3084. [\[CrossRef\]](#)
12. Newell, S.; Goggins, J. Experimental Study of Hybrid Precast Concrete Lattice Girder Floor at Construction Stage. *Structures* **2019**, *20*, 866–885. [\[CrossRef\]](#)
13. Chen, Y.; Shi, H.-R.; Wang, C.-L.; Wu, J.; Liao, Z.-Q. Flexural Mechanism and Design Method of Novel Precast Concrete Slabs with Crossed Bent-up Rebar. *J. Build. Eng.* **2022**, *50*, 104216. [\[CrossRef\]](#)
14. Qi, J.; Yang, H.C. Improvement of a Truss-Reinforced, Half-Concrete Slab Floor System for Construction Sustainability. *Sustainability* **2021**, *13*, 3731. [\[CrossRef\]](#)
15. Yardim, Y.; Waleed, A.M.T.; Jaafar, M.S.; Laseima, S. AAC-Concrete Light Weight Precast Composite Floor Slab. *Constr. Build. Mater.* **2013**, *40*, 405–410. [\[CrossRef\]](#)
16. Li, S.; Chen, W.; Zhang, Y. Flexural Behavior of Precast, Prestressed, Lightweight Aggregate Concrete-Conventional Concrete Composite Beams. *Constr. Build. Mater.* **2021**, *274*, 121926. [\[CrossRef\]](#)
17. Aarathi, D.K.; Jeyshankaran, E.; Aranganathan, N. Comparative Study on Longitudinal Shear Resistance of Light Weight Concrete Composite Slabs with Profiled Sheets. *Eng. Struct.* **2019**, *200*, 109738. [\[CrossRef\]](#)
18. Ahmed, I.M.; Tsavdaridis, K.D. Shear Connection of Prefabricated Slabs with LWC—Part 1: Experimental and Analytical Studies. *J. Constr. Steel Res.* **2020**, *169*, 106016. [\[CrossRef\]](#)
19. Lv, J.; Zhou, T.; Wu, H.; Sang, L.; He, Z.; Li, G.; Li, K. A New Composite Slab Using Crushed Waste Tires as Fine Aggregate in Self-Compacting Lightweight Aggregate Concrete. *Materials* **2020**, *13*, 2551. [\[CrossRef\]](#)
20. Zhu, Y.; Zhang, Y.; Hussein, H.H.; Chen, G. Flexural Strengthening of Reinforced Concrete Beams or Slabs Using Ultra-High Performance Concrete (UHPC): A State of the Art Review. *Eng. Struct.* **2020**, *205*, 110035. [\[CrossRef\]](#)
21. Lee, M.-G.; Wang, Y.-C.; Chiu, C.-T. A Preliminary Study of Reactive Powder Concrete as a New Repair Material. *Constr. Build. Mater.* **2007**, *21*, 182–189. [\[CrossRef\]](#)
22. Kang, S.-T.; Lee, Y.; Park, Y.-D.; Kim, J.-K. Tensile Fracture Properties of an Ultra High Performance Fiber Reinforced Concrete (UHPC) with Steel Fiber. *Compos. Struct.* **2010**, *92*, 61–71. [\[CrossRef\]](#)
23. Yoo, D.-Y.; Shin, H.-O.; Yang, J.-M.; Yoon, Y.-S. Material and Bond Properties of Ultra High Performance Fiber Reinforced Concrete with Micro Steel Fibers. *Compos. Part B Eng.* **2014**, *58*, 122–133. [\[CrossRef\]](#)
24. Luo, J.; Zheng, L.; Pei, B.; Wang, Y.; Yan, H.; Zhao, J. Key Design Parameters Analysis and Calculation Theory Research on Bending Performance of Steel—UHPC Lightweight Composite Deck Structure. *Buildings* **2023**, *13*, 504. [\[CrossRef\]](#)
25. Cai, H.; Liu, Z.; Xu, Z.; Zhang, Z.; Xu, T. Flexural Tensile Behavior of Interface between Precast and Cast-in-Place UHPC Members Based on Four-Point Bending Test. *Buildings* **2023**, *13*, 745. [\[CrossRef\]](#)
26. Prasittisopin, L.; Termkhajornkit, P.; Kim, Y.H. Review of Concrete with Expanded Polystyrene (EPS): Performance and Environmental Aspects. *J. Clean. Prod.* **2022**, *366*, 132919. [\[CrossRef\]](#)
27. ASTM C39; Concrete Cylinder Compression Testing. ASTM International: West Conshohocken, PA, USA, 2005.
28. ASTM C496/C496M-04; Standard Test Method for Splitting Tensile Strength of Cylindrical Concrete Specimens 2017. ASTM International: West Conshohocken, PA, USA, 2017.
29. Sun, J.; Li, R.Y.M.; Jiao, T.; Wang, S.; Deng, C.; Zeng, L. Research on the Development and Joint Improvement of Ceramsite Lightweight High-Titanium Heavy Slag Concrete Precast Composite Slab. *Buildings* **2023**, *13*, 3. [\[CrossRef\]](#)

30. Feng, Y.; Qi, J.; Wang, J.; Liu, J.; Liu, J. Flexural Behavior of the Innovative CA-UHPC Slabs with High and Low Reinforcement Ratios. *Adv. Mater. Sci. Eng.* **2019**, *2019*, 6027341. [[CrossRef](#)]
31. *ACI CODE-318-19*; Building Code Requirements for Structural Concrete and Commentary 2019. ACI Committee: Farmington Hills, MI, USA, 2019.
32. *ACI 544.4R-88*; Design Considerations for Steel Fiber Reinforced Concrete. ACI Committee: Farmington Hills, MI, USA, 1999; Volume 88, p. 18.

Disclaimer/Publisher's Note: The statements, opinions and data contained in all publications are solely those of the individual author(s) and contributor(s) and not of MDPI and/or the editor(s). MDPI and/or the editor(s) disclaim responsibility for any injury to people or property resulting from any ideas, methods, instructions or products referred to in the content.